Phytomedicine Plus 2 (2022) 100216

Contents lists available at ScienceDirect

Phytomedicine Plus

journal homepage: www.sciencedirect.com/journal/phytomedicine-plus

# Glycogen synthase kinase 3β inhibition and insulin-receptor binding enhancement of compounds isolated from wild leafy vegetable *Acalypha alnifolia*

Revathi Ponnusamy [a,*], Kalaiarasi Giriraj [b], Magesh Selvakumar AM [c], Parimelazhagan Thangaraj [d,*], Saikumar Sathyanarayanan [e], Adriano Antunes de Souza Araújo [f], Saravanan Shanmugam [f,*], Lucindo José Quintans Junior [f]

[a] PG and Research Department of Botany, Kongunadu Arts and Science College (Autonomous), Coimbatore 641 029, India
[b] Department of Chemistry, Karpagam Academy of Higher Education (Deemed to be University), Coimbatore, Tamil Nadu 641 021, India
[c] Department of Chemistry, Bharathiar University, Coimbatore, Tamil Nadu 641 046, India
[d] Department of Botany, Bharathiar University, Coimbatore, Tamil Nadu 641 046, India
[e] Department of Botany, PSG College of Arts and Science, Coimbatore, Tamil Nadu 641 014, India
[f] Department of Pharmacy, Federal University of Sergipe, Av. Marechal Rondon, Jardim Rosa Elze, Sao Cristovao, Sergipe 49100-000, Brazil

ARTICLE INFO

*Keywords:*
Acalypha alnifolia
Isokaempferide
Glycogen synthase kinase 3β
Insulin receptor
Pyridine alkaloid

ABSTRACT

*Background:* The traditional information of *Acalypha alnifolia* is captivate towards its therapeutic efficacy against diabetes along with the scientific confirmation were leads to an instinct to extract phytocompounds and to evaluate antidiabetic-molecular mechanism.
*Methods:* Column chromatographic compound isolation were adopted to extract the pure compounds from bioactive leaf extract and interactions of the compounds with diabetic metabolic proteins were accomplished through *in-silico* docking studies. By the direction, the anti-diabetic property was valued by the expressions of Glycogen Synthase Kinase 3β(GSK 3β) and Insulin on insulin-Receptor on Hep G2 cells.
*Results:* The flavone compound - 5,7-dihydroxy-2-(4-hydroxyphenyl)-3-methoxy-4*H*-chromen-4-one and pyridine alkaloid - (2,6-dihydroxypyridin-4-yl)(3,5-dihydroxytetrahydro-2*H*-pyran-4-yl) acetic acid were isolated. Both the compounds reduced the GSK 3β expression and the flavone contributed also to enhance insulin binding ability expediently.
*Conclusions:* The results concluded that the compounds from *A. alnifolia* having potent to maintain glucose homeostasis in liver insulin-metabolism. By exploring pharmaceutical importance of the isolated compounds, this study will be an important breakthrough in developing new drug for Diabetes.

## 1. Introduction

Management of Diabetes is still a challenge for the clinician and the complexity of Diabetes and its impact on whole body homeodynamics are two of the main reasons why there is not yet such a drug. Moreover, the molecular mechanisms by which Diabetes can be controlled are still under an intense debate (Meneses et al., 2015). Researchers are exploring safe and effective medications to overcome the detrimental effects of insulin resistance-related metabolic derangement, including hyperglycaemia, hyperinsulinaemia, hyper-lipidaemia, oxidative stress, inflammation, atherosclerosis and other complications (Defronzo et al., 2013).

In present study, the underutilized and narrow explored plant *Acalypha alnifolia* have chosen for compound isolation and to evaluate the efficiency of compounds against diabetes. As well, the plant *A. alnifolia* belongs to the family Euphorbiaceae, traditionally used as a leafy vegetable and to treat hypertension (Johnkennedy et al., 2011), skin problems (Ponnusamy and Thangaraj, 2014), diabetes (Balakrishnan et al., 2009). The research reports conveying, it has *in vitro* and *in vivo* antioxidant potential (Evanjelene and Natarajan, 2012) and suggested that the high polar solvent extracts showed better antioxidant ability. Additionally, splendid secondary metabolites such as total phenolics,

* Corresponding authors.
*E-mail addresses:* revathip_bo@kongunaducollege.ac.in (R. Ponnusamy), drparimel@gmail.com (P. Thangaraj), saranflora04@gmail.com (S. Shanmugam).

https://doi.org/10.1016/j.phyplu.2022.100216
Received 20 August 2021; Received in revised form 25 December 2021; Accepted 7 January 2022
Available online 10 January 2022

flavonoids, and tannin contents were found in acetone extract of *A. alnifolia*, (Revathi and Parimelazhagan, 2015a). It also has a perfect nutritional composition; the acetone and methanol extracts possessed significant analgesic, anti-inflammatory, antipyretic properties (Ponnusamy and Thangaraj, 2014) and acetone extract has better anti-diabetic properties (Revathi and Parimelazhagan, 2015a) in the animal model. This information on studied plant supports the hypothesis that antioxidants from plant-based and natural products with strong anti-diabetic, anti-inflammatory and antiglycative properties are emerging as a future therapy. As opposed to conventional medications, antioxidants may be an alternative and beneficial way to prevent and treat this life-threatening disease (Mohamed et al., 2016).

Glucose homeostasis is tightly regulated to meet the energy requirements of the vital organs and maintain an individual's health. The liver has a major role in the control of glucose homeostasis by controlling various pathways of glucose metabolism, including glycogenesis, glycogenolysis, glycolysis and gluconeogenesis (Han et al., 2016). On feeding, increased insulin signaling activates Protein kinase B (PKB), in the cell, which in turn phosphorylates and inactivates GSK-3 (Glycogen synthase kinase-3), thus resulting in the activation of glycogen synthase (Suzuki et al., 2013).

Insulin is the mainstay therapy of type 1 diabetes, whereas agents that increase insulin secretion or activity are the primary approaches to therapy of type 2 diabetes. First line conventional therapies for type 2 diabetes include biguanides (metformin) and sulfonylureas. Metformin increases insulin sensitivity whereas the sulfonylureas increase insulin secretion. The overexpression of GSK-3 has been shown to attenuate insulin signaling due to phosphorylation and downregulation of insulin receptor substrate-1 (Sharfi and Eldar-Finkelman, 2008). Therefore, it has been suggested that drugs inhibiting GSK-3 could mimic the ability of insulin to promote the conversion of glucose to glycogen, overcoming the resistance to insulin (Nabben and Neumann, 2016; Sepidarkish, et al. 2020).

Current therapies although effective, are not without limitations. Along with these limitations, the alarming increase in the prevalence of diabetes, and soaring cost of managing diabetes and its complications underscores an urgent need for safer, more efficient and affordable alternative treatments (Lankatillake et al., 2019). Hence, based on these requirements, the compound isolation from acetone extract of wild leafy vegetable and antidiabetic plant *Acalypha alnifola* to confine glucose homeostasis efficiency of isolated compounds on docking directed proteins are aimed in the present study.

## 2. Materials and methods

### 2.1. Chemicals

All the solvents used were of the highest purity (>99.5%) and analytical grade (Merck) made in India. Other chemicals were purchased from Sigma–Aldrich (St. Louis, MO, USA).

### 2.2. Collection and extraction of plant material

The plant *A. alnifolia* was collected from the Bharathiar University campus and Madhukarai Dharmalingeswara hills, Coimbatore, India. The plant was identified and authenticated by the Botanical Survey of India, Southern Circle, Coimbatore, India (authentication number BSI/SRC/5/23/2011–12/Tech.−1137) and the voucher specimen was deposited in Bharathiar Herbarium, Department of Botany, Bharathiar University (Voucher no. 006302). The leaves were separated from the plant, washed in running tap water, shade-dried and powdered. This powdered sample was taken for successive solvent hot percolation extraction with petroleum ether, chloroform, acetone, and methanol using the Soxhlet apparatus (Agarwal et al., 2012).

### 2.3. Selection of extract and solvents for compound isolation

The plant *A. alnifolia* leaf acetone extract reported having a better quantity of secondary metabolites, very good antioxidant and pharmacological potential includes analgesic, anti-inflammatory, hypoglycemic, hypolipidemic, antidiabetic properties (Ponnusamy and Thangaraj, 2014; Revathi et al., 2013; Revathi and Parimelazhagan, 2015b). Since the isolation of active compounds from the better extract is the main objective, acetone extract has been taken for compound isolation. The wet pack of silica gel was prepared with petroleum ether. According to the previous isolation research reports, the solvents such as chloroform and ethyl acetate were chosen as eluent.

### 2.4. Column chromatographic compound isolation

The column has been prepared by using 60–120 mesh silica gel. The column size is about 50 cm x 30 mm. The *A. alnifolia* acetone extract of about 15 g was packed with 30 g of silica gel. Initially, it eluted with petroleum ether and followed by chloroform and by ethyl acetate. The solvent concentration has gradually increased by 5%. The eluted fractions were collected in separate test tubes that were about 10 mL approximately and concentrated. The elutions were tested to travel on Thin Layer Chromatography (TLC); the same distance traveled by the elutions in the same mobile phase was poured together and each has been taken for further structural analysis (Bajpai et al., 2016).

### 2.5. Thin layer chromatography

The *A. alnifolia* acetone extract was selected for purifying compounds on a random isolation basis. The selection of the extract was made based on the activity shown both *in vitro* and *in vivo* experiments. The preliminary chemical profiling of fractions with maximum antioxidant activity were screened using thin layer chromatography. TLC profiling was done on pre-coated silica gel 60 GF254 TLC plate (Merck, Ponda, Goa, India). The chromatogram was developed in a saturated chromatographic chamber. The developed plate was visualized under UV chamber and iodine chamber (Bajpai et al., 2016; Thangaraj, 2016) .

### 2.6. Fourier transform infra-red spectroscopy (FTIR) and nuclear magnetic resonance (NMR)

FT-IR spectrometer (Shimadzu) outfitted with a ceramic source, KBr bar splitter. Infrared spectra of *A. alnifolia* acetone extract were recorded on an IR Tracer-100 (Shimadzu) Fourier Transform Infrared Spectrophotometer, at room temperature. Spectrum infrared absorption was obtained in the range of 4000–500 $cm^{-1}$in KBr pellets. The unique spectrum of natural compound can be generated and structural clarification, mainly used infrared (IR), radio frequency (FT-IR), and electron beam (Popova et al., 2009) 2009.

The NMR technique is important to elucidate the $^{1}H$ NMR and $^{13}C$ NMR analysis were performed on the Varian VNMRS spectrometer. Samples will be diluted in DMSO-$d_6$ at 25°C in 5 mm tubes. Chemical variations were shown in ppm using DMSO-$d_6$ (2.50 ppm) as the internal standard.

### 2.7. Antioxidant activity: DPPH (2,2-diphenyl-1-picrylhydrazyl) radical scavenging activity and ABTS (2, 2 – azinobis (3- ethylbenzothiazoline- 6-sulphonic acid) radical cation scavenging assay

The antioxidant activity of the screened elution was determined using the stable radical DPPH according to the method of Blois, 1958). Radical scavenging activity of the samples was conveyed as $IC_{50}$ i.e., the sample concentration required to inhibit 50% of $DPPH^{\bullet}$ concentration. The total antioxidant activity was measured by ABTS radical cation decoloration assay according to Re et al. (1999). The inhibition was calculated against the blank with absorbance at 734 nm. The unit of total

antioxidant activity was defined as the concentration (μg) of Trolox equivalent antioxidant activity in a gram of sample.

### 2.8. In-silico study

#### 2.8.1. Glucose homeostasis proteins for docking study

The extracted and structure identified compounds were accomplished by Glide extra precision (XP) docking with the glucose homeostasis proteins such as Peroxisome Proliferator-Activated Receptor (alpha and gamma) [PPAR (α and γ)], Insulin Receptors (IR), Protein Tyrosine Phosphatase 1 Beta (PTP 1β), Dipeptidyl peptidase 4 (DPP 4), Glycogen Synthase Kinase-3β (GSK-3β), Aldose Reductase (AR). The docking provides G-score, the number of H bonds interacting with active sites of selected protein, and the bond length has been evaluated and compared with standard drugs. The standard drug Glibenclamide has been taken for comparison (Panchal et al., 2018).

#### 2.8.2. Retrieval of target structures and preparation of ligands

The three-dimensional structures of the target proteins were copied from the Protein Data Bank (PDB). The structures of isolated compounds were built by using ChemSketch. The reference drug molecule Glibenclamide was obtained from the PubChem database. The ligands were equipped with Ligrep software ( Kim, 2016;Pagadala et al., 2017).

#### 2.8.3. Molecular docking and prediction of ADMET (absorption, distribution, metabolism, excretion, and toxicity) properties

Retrieved protein structures were subjected to removal of water up to 5 Å distances, assigning lone pair electron atom using protein preparation wizard. The receptor grid was set up and generated to specify the binding pocket where the ligand binds using the Receptor Grid Generation panel. The opls_5 force field was used. Molecular docking of the prepared RNA and the ligands was conceded using GLIDE. The ADMET properties of the ligand compounds were determined using Qikprop to assess their drugability. This study estimates the aqueous solubility of the ligands and blood-brain barrier penetration (BBB) primarily. The acceptability and drug-ability of the compounds were also evaluated based on Lipinski's rule of 5 (Lipinski, 2001; Lipinski et al., 2001).

### 2.9. Cell line study

The Hep G2 liver cell line [American Type Culture Collection (ATCC)] has engaged with the isolated compounds and observed the cytotoxicity, expressions of GSK 3β proteins, and the effect of insulin binding capability with insulin receptors using fluorescence flow cytometer. Cytotoxicity of the isolated compounds was analyzed (Mosmann, 1983) and the linear regression equation determined values ($IC_{50}$).

### 2.10. Glycogen synthase kinase 3β (GSK 3β) inhibition activity

Culture cells in a 6-well plate at a density of $3 \times 10^5$ cells/2 mL were incubated in a $CO_2$ incubator overnight at 37°C for 24 h. The spent medium was aspirated and washed with 1 mL 1X PBS. The cells were treated with a required concentration of experimental compounds and control in 2 mL of culture medium and incubated for 24 h. At the end of the treatment, the medium was removed out from all the wells and washed with 500 μL of PBS (Phosphate-buffered saline). The removed PBS was saved in the respective polystyrene tube and 180μL of the trypsin-EDTA(trypsin-Ethylenediamine tetraacetic acid) solution was added and again incubated for 3–4 min. The culture medium was poured back into their respective wells and harvested the cells directly into polystyrene tubes. The tubes were centrifuged for five minutes at 300 x *g* at 25°C. Carefully the supernatant was decanted. After PBS wash (twice) 0.5 mL of 2%, the Paraformaldehyde solution was added and incubated for 20 min. The cell culture was washed with 0.5% bovine serum albumin (BSA) in PBS. Then 0.1% Triton-X100 in 0.5% BSA solution was added and incubated for 10 min. Again the cell culture wells were washed with BSA and the GSK 3β Tyr279+Tyr216, FITC (Fluorescein isothiocyanate) conjugated antibody (1:50) was added. The cell culture was incubated for 30 min in the dark at room temperature. Finally, again washed with PBS and added 0.5 mL of PBS, mixed thoroughly just before analysis. The fluorescence emissions were observed by flow cytometry [FACS (fluorescence-activated cell sorting) Calibur] using 488 nm laser for excitation and 535 nm laser for detection (FL1) (Melan, 1999; Amidzadeh et al., 2014).

### 2.11. Insulin receptor (IR) binding activity

Culture cells are maintained and treated with compounds like the previous protocol. At end of the treatment, the Insulin - Fluorescent Isothiocyanate (Insulin-FITC) 100 nM was added and incubated for 30 min. The medium was removed from all the wells into polystyrene tubes and washed twice with 500μL PBS. The PBS was removed and added 500μL of 0.5 mM EDTA (Ethylenediaminetetraacetic acid) solution and incubated at 37°C for 10 min. The culture medium was poured back into their respective wells and harvested the cells directly into polystyrene tubes kept at 4–8°C. The tubes were centrifuged for five minutes at 300x *g* at 4–8°C and carefully, the supernatant was decanted. The cells were resuspended in 500μL PBS and analyzed by flow cytometry (FACS Calibur) using the 488 nm laser for excitation and detection at 535 nm (Forward Light Scatter-FL1) (Qiang et al., 2014).

### 2.12. Statistical analyses

The results of antioxidant and protein expression study on liver cells were expressed as Mean ± Standard Deviation (SD).

## 3. Results

### 3.1. Column chromatographic compound isolation

Forty elutions have obtained from petroleum ether:chloroform mobile phase and chloroform:ethyl acetate mobile phase (each twenty). Out of which, five were selected according to their DPPH (2,2-diphenyl-1-picrylhydrazyl) radical scavenging ability such as

1. 20% ethyl acetate: 80% chloroform - 145 mg - DPPH $IC_{50}$ @ 50 μg/mL (24th elution);
2. 40% ethyl acetate: 60% chloroform – 18 mg - DPPH $IC_{50}$ @ 30 μg/mL (28th elution);
3. 45% ethyl acetate: 55% chloroform – 21 mg (crystal)- DPPH $IC_{50}$ @ 5 μg/mL (29th elution);
   a. 90% ethyl acetate: 10% chloroform - 78 mg (beads) - DPPH $IC_{50}$ @ 12 μg/mL (38th A elution);
   b. 90% ethyl acetate: 10% chloroform - 60 mg - DPPH $IC_{50}$ @ 10 μg/mL (38th B elution)
4. 100% ethyl acetate – 72mg- DPPH $IC_{50}$ @ 8 μg/mL (40th elution);

The semi-crystalline compound was acquired from 45% ethyl acetate elution on dry. The bead like separation from bottom brown sticky substance was observed in 90% ethyl acetate elution and was collected in tubes. As a final 29th elution and part of 38th elution has been stunted for further purification and characterization.

### 3.2. Purification of selected compounds

The fraction with good activity was reserved for TLC and pure fractions were taken into Fourier Transform Infra-Red Spectroscopy (FTIR) and Nuclear Magnetic Resonance (NMR) spectroscopic structure elucidation. Initially, the 45% ethyl acetate elution appeared like a crystalline compound whereas 90% ethyl acetate elution (38 A) was a white layer. The TLC mobility of both elutions spotted a single band that

was confirmed their purity.

1 45% ethyl acetate elution; Mobile Phase– Ethyl acetate: methanol (90:10); Distance traveled by Solvent Front: 4.5; Distance traveled by compound: 3.3; $R_f = 0.73$;
2 90% ethyl acetate elution: Mobile Phase –Ethyl acetate: methanol (75:25); Distance traveled by Solvent Front: 5; Distance traveled by compound: 4; $R_f = 0.80$

The purity of 45% elution was attained by pouring in watch glass, dissolving in a subsequent solvent, and casting out the clear semi-crystalline compound on dry. The remaining impure suspension on watch glass was again dissolved and left for dry, and then the pure semi-crystalline substance was scrapped and stored. Likewise, the 90% ethyl acetate elution was purified by collecting the white substances without debris by dissolving in ethyl acetate and separated for several times. Both purified substances were measured and stored for the characterization and further studies.

### 3.3. Fourier transform infra-red spectroscopy (FT-IR) and nuclear magnetic resonance (NMR)

The characterization of the compounds was done by using FT-IR and NMR spectroscopic techniques. The spectrum of both the effective elution with purity was undertaken for structure elucidation. Infrared spectroscopy predicts active compounds by the peaks due to the vibrational excitation of covalently bonded atoms and groups. Their ranges like 1600cm$^{-1}$, 2900cm$^{-1}$, and 3400cm$^{-1}$ indicate the presence of C=O, C—H, and -O—H, respectively. In addition to these functional groups, in 90% ethyl acetate fraction a peak range 3200cm$^{-1}$ indicates the presence of C—N. The above-mentioned functional groups corresponding with the NMR spectrum, the structure of the pure compounds have predicted accordingly. The compound images are shown in Fig. 1 for compound 1 and Fig. 2 for compound 2.

The IR spectral band of compound 1 showed the band at 1692cm$^{-1}$, which revealed that the compound contained the lactone group. The characteristic absorption band corresponding to the presence of the C—O group was observed at 1330cm$^{-1}$. The broadband was observed at 3402cm$^{-1}$ corresponding to the –OH group. The infrared spectroscopic analysis of isolated compound 2 showed broadband at 3483cm$^{-1}$ corresponding to the –OH group and a sharp band observed at 3221cm$^{-1}$ due to an -NH stretching. The bands observed at 1684cm$^{-1}$ and 1647cm$^{-1}$ corresponded to the C=O group and C=N group, respectively. The aromatic and aliphatic C-H stretching was observed in the expected region in both compounds.

The $^{1}$H—NMR spectroscopic technique revealed the presence of one broad singlet at the most downfield value δ 12.19 ppm for the proton attached to an oxygen atom in compound 1. Broad singlet observed at δ 9.16 and δ 8.81 ppm corresponding to the -OH group. Multiplets observed at δ 6.63–7.31 ppm assigned to the aromatic protons. A sharp singlet was observed at δ 2.58 ppm due to the methoxy group. In compound 2, one broad singlet at δ 12.85 ppm corresponds to the acid group proton. The multiplet observed at δ 6.65–6.83 ppm was assigned to the aromatic protons. Two aromatic -OH protons were observed at δ 4.89 ppm. Two aliphatic -OH protons were observed at δ 4.03 ppm. Two singlets observed at δ 3.68 and δ 3.71 ppm were assigned to methylene group protons. A singlet was observed at δ 3.34 ppm assigned to the CH protons coupled with -OH proton. In addition, CH proton exhibited a singlet at δ 2.73 ppm.

The $^{13}$C—NMR spectroscopic analysis of isolated compound 1 showed signals corresponded to all the carbons in the compound. Signals at δ 183.91 ppm could be assigned to the C=O group. The methoxy carbon was found to resonate upfield at δ 63.26 ppm. The peak corresponding to the C—OH group was observed at δ 167.91, δ 165.73, δ 163.35 and δ 152.25 ppm. The rest of the aromatic carbons were found to resonate in the expected region. In compound 2, signals at δ 67.03 and δ 71.36 ppm could be assigned to the C—O group. The CH—OH carbon was found to resonate at δ 65.94 and δ 74.56 ppm, whereas C—OH carbon was found to resonate at δ 159.98 and δ 163.39 ppm. Signals at δ 168.68 ppm could be assigned to COOH carbon and aliphatic CH carbons were observed in the expected region. Based on the spectral data obtained, the compound 1 is 5,7-dihydroxy-2-(4-hydroxyphenyl)−3-methoxy-4*H*-chromen-4-one and compound 2 is (2, 6-dihydroxypyridin-4-yl) (3,5-dihydroxytetrahydro-2*H*-pyran-4-yl).

### 3.4. Spectroscopic characterization

#### 3.4.1. Compound 1: (Fig. 1)

Yield = 0.14%. Mp: > 300°C. FT-IR (ν, cm$^{-1}$) in KBr: (-OH) 3400, (C=O) 1692, (C—O) 1330; $^{1}$H NMR (400 MHz, DMSO-d$_6$, δ ppm, *J Hz*): δ 12.19 (1H, s, -OH); 9.16 ($^{1}$H, s, -OH); 8.81(1H, s, -OH); 6.63–7.31 (6H, m, phenyl protons); 2.58 ($^{1}$H, s, -OCH$_3$); $^{13}$C (DMSO-d$_6$, δ ppm): 183.91 (C=O), 167.91 (C—OH), 165.73(C—OH), 163.35 (C—O), 152.25 (C—OH), ({δ 138.23, δ 139.61, δ 134.98, δ 130.08, δ 120.91, δ 109.18, δ 103.18, δ 102.26, δ 93.39, δ 86.27} aromatic protons), δ 63.26 ppm (O—CH$_3$).

#### 3.4.2. Synonyms for semi-crystalline compound (Compound 1)

5,7-dihydroxy-2-(4-hydroxyphenyl)−3-methoxy-4*H*-1-benzopyran-4-one; 5,7-dihydroxy-2-(4-hydroxyphenyl)−3-methoxy-4*H*-chromen-4-one; 5,7-dihydroxy-2-(4-hydroxyphenyl)−3-methoxychromen-4-one; Isokaemferide; Kaempferol-3-methyl ether; 3-methoxyapigenin; 3-methyl kempferol are the other names of compound 1 which was extracted and reported with many pharmacological properties in various plants.

#### 3.4.3.Compound. 2: (Fig. 2)

Yield = 0.52%. Mp: > 160°C. FT-IR (ν, cm$^{-1}$) in KBr: (OH) 3483, (NH) 3384,3221, (C=O) 1684, (C=N) 1647; $^{1}$H NMR (400 MHz, DMSO-d$_6$, δ ppm, *J Hz*): 12.85 (1H, s, -COOH); 6.83, 6.81, 6.65(3H, s, phenyl protons); 4.89 (2H, s, aromatic -OH); 4.03(2H, s, -OH); 3.71, 3.68 (4H, s, -CH$_2$), 3.34 (2H, s, -CHOH), 2.73 (1H, s, -CH); $^{13}$C (DMSO-d$_6$, δ ppm): 30.27(aliphatic CH), 37.23 (aliphatic CH), 65.94 (CH—OH), 67.03(C—O), δ 71.36(C—O), 74.56(CH—OH),{(δ 129.36, δ 137.42, δ 142.29) aromatic protons}, 159.98(C—OH), 163.39 (C—OH), 168.68 ppm (-= COOH).

#### 3.4.4.New. compound: pyridine alkaloid

Compound 2 is predicted as (2,6-dihydroxypyridin-4-yl)-(3,5-dihydroxytetrahydro-2*H*-pyran-4-yl) acetic acid which is a pyridine alkaloid. The structure of this compound is with chair conformation has good antioxidant properties but next to Isokeampferide (compound 1). This pyridine alkaloid is new to the plant chemistry as well as the present findings of bioactive compounds are the first report from this plant *A. alnifolia* which is also making curiosity to characterize and to trace pharmacological properties profoundly.

### 3.5. Antioxidant properties of isolated compounds

The antioxidant capability of both the compounds was evaluated and compared with the source extract (acetone extract of leaf) from which it was extracted and purified. Compound 1 strongly inhibited the DPPH radical by the minimum IC$_{50}$ of 5.76 μg/mL, whereas compound 2 inhibited by IC$_{50}$ of 11.29 μg/mL. An excellent ABTS$^{+}$ radical scavenging ability was observed in compound 1 (67,362.66 μg Trolox eq./g extract), which is far better than source extract (39,854.17 μg Trolox eq./g extract) and compound 2 (9520.259 μg Trolox eq./g extract). In the present study, Isokaempheride (compound 1) has efficient free radical scavenging ability than compound 2; therefore synergistically the acetone crude extract might have contributed to efficient antioxidant and pharmacological capabilities.

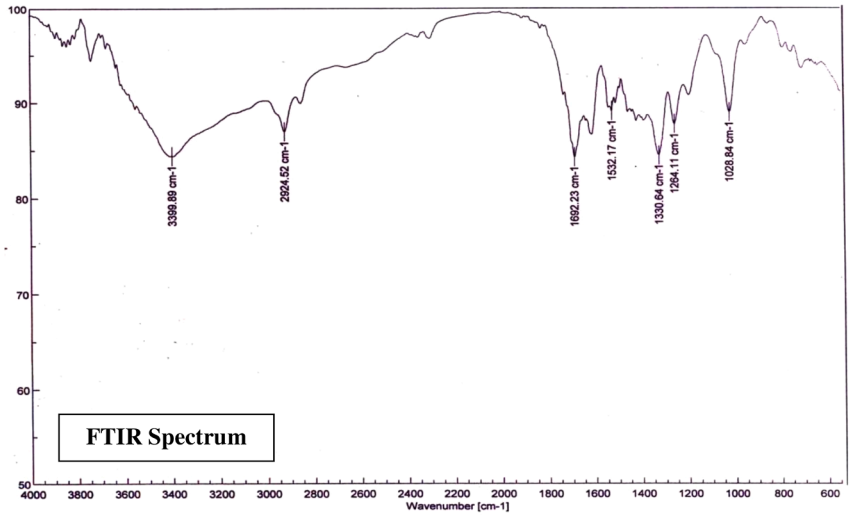


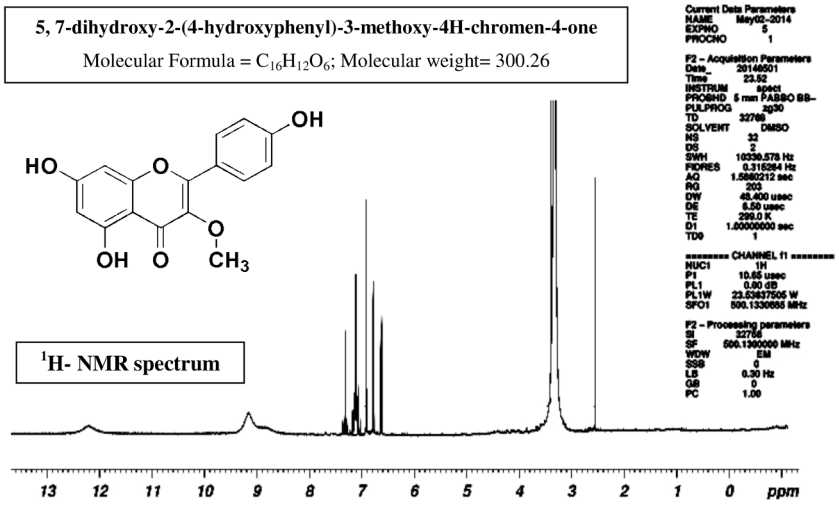


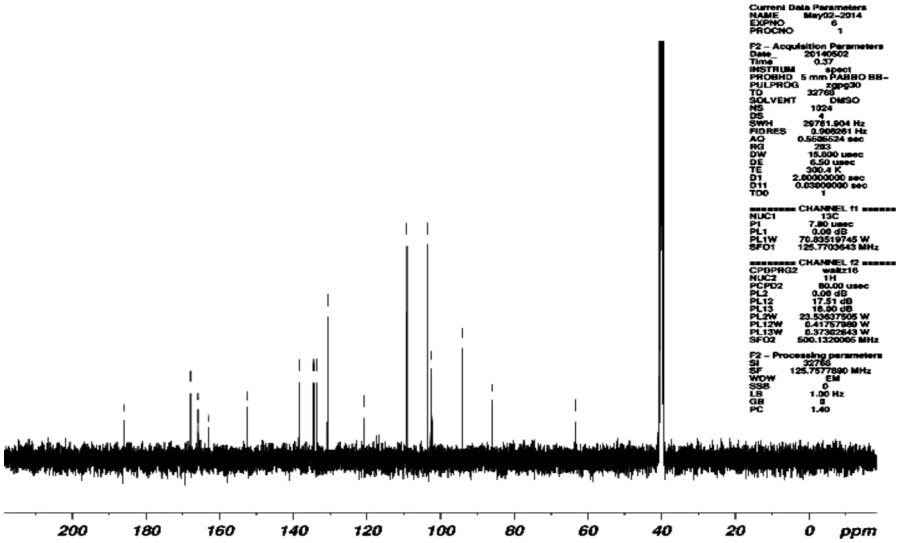


**Fig. 1.** Spectra of Compound 1 and structure. Name of the compound: 5,7-dihydroxy-2-(4-hydroxyphenyl)–3-methoxy-4*H*-chromen-4-one; Molecular Formula = $C_{16}H_{12}O_6$ Molecular weight= 300.26. FT-IR spectrum of compound 1: 3400 (-OH); 1692 (-C=O), 1692 (-C-O); $^{1}$H- NMR spectrum: 12.19 (1H, s, -OH); 9.16 (1H, s, -OH); 8.81(1H, s, -OH); 6.63–7.31(6H, m, phenyl protons); 2.58 (3H, s, –$OCH_3$); $^{13}$C -NMR spectrum: 183.91, 167.91, 165.73, 163.35, 152.25, 138.23, 139.61, 134.98, 130.08, 120.91, 109.18, 103.18, 102.26, 93.39, 86.27, 63.26.

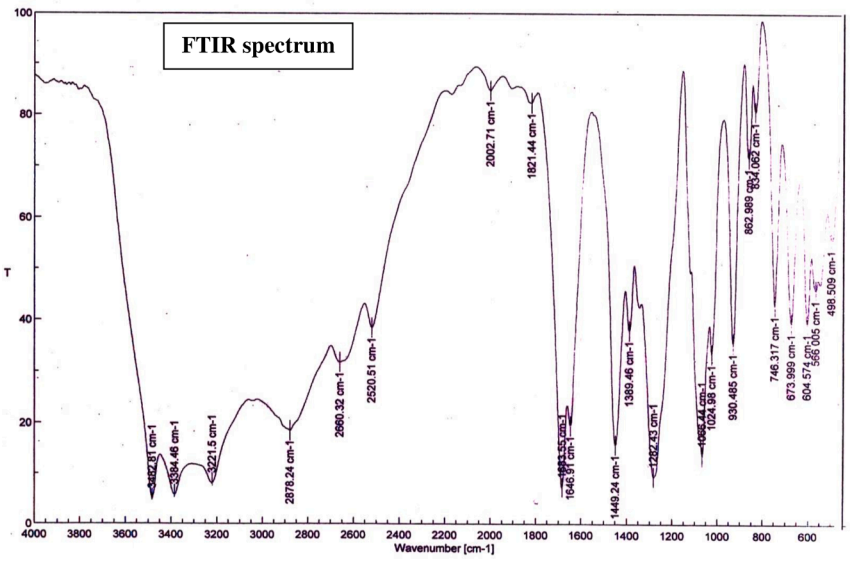


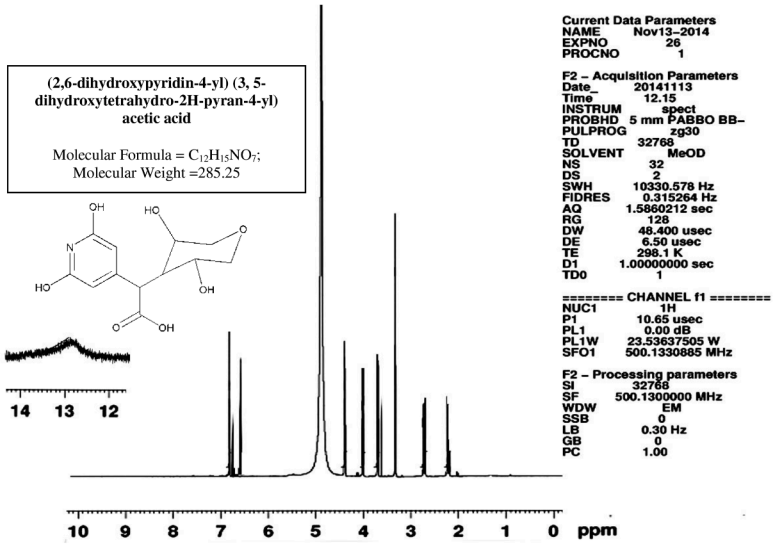


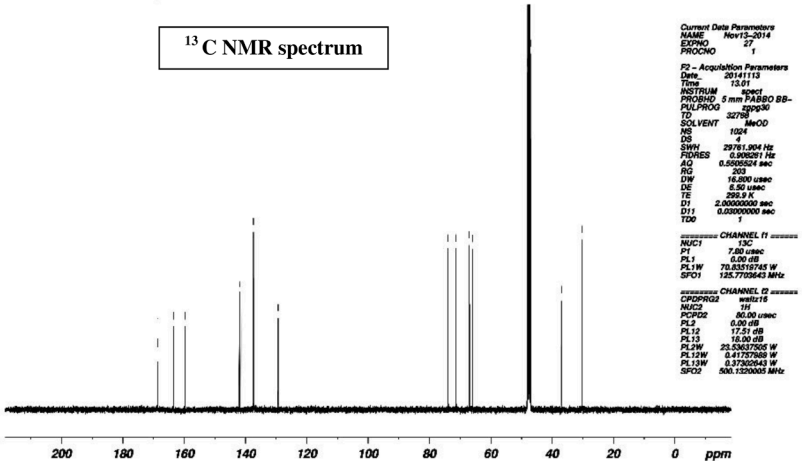


**Fig. 2.** Spectra of Compound 2 and structure. Name of the compound: (2, 6-dihydroxypyridin-4-yl)(3, 5-dihydroxytetrahydro-2*H*-pyran-4-yl) acetic acid; Molecular Formula = $C_{12}H_{15}NO_7$; Molecular Weight =285.25. FT-IR spectrum of compound 2: 3483 (-OH); 3384, 3221 (-NH); 1684 (-C=O); 1647 (-C=N); $^{1}$H- NMR spectrum: 12.85 (1H, s, -COOH); 6.83, 6.81, 6.65(3H, s, phenyl protons); 4.89 (2H, s, aromatic -OH); 4.03(2H, s, -OH); 3.71, 3.68 (4H, s, -$CH_2$), 3.34 (2H, s, -CHOH), 2.73 (1H, s, -CH); $^{13}$C -NMR spectrum: 30.27, 37.23, 65.94, 67.03, 71.36, 74.56, 129.36, 137.42, 142.29, 159.98, 163.39, 168.68.

### 3.6. Molecular docking study

Both the phytochemical ligands (Compounds) showed good interaction with all the targets than the active drug (Glibenclamide). The better interaction was considered with the least glide score and good HB (Hydrogen Bond) number, which might have influenced the particular protein levels and activity in metabolism. The interaction between the compounds and selected proteins are tabulated (Table 1). In the case of compound 1, the number of hydrogen bonds was high with PPAR γ (4 HB) and IR (4 HB). Similarly, A better binding nature was observed in Compound 2 where the number of hydrogen bonds was higher with PTP 1β (8 HB), AR (7 HB), followed by IR (6HB). The standard Glibenclamide has five hydrogen bonds with PTP 1β and there was only 3 HB found with IR followed by AR (2 HB).

Literatue explores that IR is one of the tyrosine kinase receptors, located on different tissues where it activates glucose transporter (GLUT4) and is directly involved in glucose homeostasis. Compounds 1 and 2 have bound with IR through 4 and 6 hydrogen bonds whereas G-score is −4.34, G-energy is −39.25 kcal/mol and G-score is −8.63, G-energy is −41.68 kcal/mol, respectively. Both the compounds have substantial docking scores with IR and medium scores with PPAR and GSK 3β proteins. Though the hydrogen bonds of compound 1 are less with GSK 3β, the glide score is least which is desirable binding nature hence the GSK 3β and IR have been carefully chosen for the molecular studies.

### 3.7. Solubility prediction (ADMET) and rule of five

The physicochemical properties such as molecular weight, hydrogen bond donors and acceptors, aqueous solubility (QP log S), octanol/water partition coefficient (QP log P), blood/brain partition coefficient (QP log BB) and human oral absorption were predicted and are shown in Table 2. Both compounds obey the Lipinski rule of 5 where the values comes within the ranges given. The compound 1 has high oral absorption (77.3%) when compared to compound 2 which shows medium oral absorption (37.3%) here less than 25% is to be considered as minimum absorption.

### 3.8. Cell line study

#### 3.8.1. Cytotoxicity

Cytotoxicity analysis was carried out in Hep G2 cell lines and by which the doses have been fixed for further experiments. At 75 μg the compound 1 has almost destroyed up to 26% of the cells in the culture. The concentration required for 50% inhibition is 97.90 μg/mL. Solidly 80% of the viable population is preferred to investigate the drug activities on living cells therefore the doses of 30 μg and 60 μg were selected for further experiments. Adherent patches of cells were observed in untreated cells. The 50% cell death was observed in commercial market drug Camptothecin (100 μM). Compound 1 has already proved its antiproliferative effect with various cell lines, whereas the present study observed the cytotoxic effect on Hep G2 cell line. The morphological changes over control diagnosed the dead cells present in the treated vials. The cells were looking clumped with black patches; appear desperation of the cell bounce. Compound 1 is inhibited the cell population gradually with concentration-dependent.

Compound 2 showed significantly less inhibition. The maximum concentration of 450 μg was destroyed only up to 18%. The $IC_{50}$ is approximately at above 700 μg. The effectiveness of compounds by their lower concentration is always appreciable therefore, random doses such as 100 μg and 200 μg of compound 2 were chosen for further experiments on Hep G2 cell line.

#### 3.8.2. Glycogen synthase kinase 3β inhibition activity of compounds 1 and 2

The GSK 3β-FITC antibody bounded with the GSK 3β of Hep G2 cells were detected by Fluorescent flow cytometry. The compound 1 and 2 treated Hep G2 cells were expressed the minimum GSK 3β. The more negligible fluorescence indicated that the inhibition of GSK 3β expression which was tabulated as Mean Fluorescent Intensity (MFI) (Table 3) particularly, the lower concentrations that are 30 μg of compound 1 and 100 μg of compound 2 inhibited the GSK 3β expression whereas 60 μg and 200 μg of respective compound 1, 2 and metformin (10 mM and 20 mM) were not involved in the inhibition and MFI was similar with untreated. Hence the lower doses of both the compounds pointedly inhibited the GSK 3β.

#### 3.8.3. Insulin receptor binding activity of compounds 1 and 2

The insulin receptors present in the treated cells were overwhelmed with insulin-FITC. The treated cells corresponded with control cell expressions for compounds 1 and 2 separately. The insulin-FITC was bounded on insulin receptors of Hep G2 cells that were detected with FACS. The high intensity of fluorescence indicated that the expression of insulin receptors by the treatment of Isokaempferide (compound 1) at particularly 60 μg/mL is desirably upright like standard metformin at their 20 mM concentration. The Mean Fluorescent Intensity (MFI) of treated cells is shown in Table 3. The geometric mean of Isokaempferide was 13.60, whereas for metformin, it was 13.82. In the case of compound 2, the lower concentration (100 μg/mL) did not alter the insulin receptor binding property, whereas the higher concentration (200 μg/mL) affected the binding nature instead.

The florescent peak of untreated cells and compounds-treated cells were compared. The treated cells peak gradually moving toward the right side due to more intensity which indicating increased insulin binding ability. The expressions of Insulin Receptors (IR) by compound 1 (Isokaempferide) treated cells were exceeded the control cells that show the considerable insulin receptor binding augmentation and is most likely to that of standard metformin expression. Isokaempferide might be bound to the receptor kinase domain of insulin receptor to trigger its kinase activity at microgram concentrations. Hence, this promising compound mimics the biological functions of insulin and is useful for further drug development for diabetic treatment.

**Table 1**
Dock score and H-bond interactions of compounds and standard glibenclamide with target proteins.

| Target proteins | PDB ID | Compound 1 G-score(kcal/mol) | G-energy(kcal/mol) | No. of Hbonds | Compound 2 G-score(kcal/mol) | G-energy(kcal/mol) | No. ofHB | Glibenclamide G-score(kcal/mol) | G-energy(kcal/mol) | No. of H bonds |
|---|---|---|---|---|---|---|---|---|---|---|
| PPAR-α | 4BCR | −6.403 | −40.881 | 2 | −7.677 | −42.255 | 4 | −2.32 | −57.332 | 2 |
| PPAR-γ | 4E4K | −8.044 | −41.91 | 4 | −7.226 | −38.992 | 2 | −8.185 | −47.418 | 2 |
| GSK-3β | 3GB2 | −7.675 | −32.023 | 2 | −8.19 | −36.895 | 4 | −5.711 | −52.036 | 1 |
| PTP-1β | 3QCG | −3.291 | −26.72 | 0 | −7.008 | −41.562 | 8 | −2.385 | −26.551 | 5 |
| DPP 4 | 3GOB | −4.606 | −34.196 | 2 | −6.571 | −39.271 | 4 | −3.711 | −48.194 | 1 |
| IR | 4XSS | −4.337 | −39.249 | 4 | −8.626 | −41.682 | 6 | −3.992 | −45.622 | 3 |
| AR | 4XZH | −6.38 | −39.45 | 1 | −12.1 | −36.69 | 7 | −2.54 | −66.65 | 2 |

PPAR- Peroxisome proliferator-activated receptor; GSK 3β- Glycogen synthase kinase 3β; PTP 1β- Protein tyrosine phosphatase-1β; DPP IV- Dipeptidyl peptidase-IV; IR-Insulin Receptor.

**Table 2**
Values of compounds 1 and 2 of *A. alnifolia* under Lipinski rule.

| S. No | Compound | Mol. wt (130–725) | Donor Hydrogen Bond (0–6) | Acceptor Hydrogen Bond (2–20) | QP log P (oct/wat) (−2.0/6.5) | QP log S (−6.5–0.5) | QP Log BB (−3.0–1.2) | Lipinski Rule of 5 violations (maximum 4) | Human oral absorption (>80% is high) |
|---|---|---|---|---|---|---|---|---|---|
| 1 | Compound 1 | 300.267 | 2.0 | 4.5 | 1.795 | −3.34 | −1.328 | 0 | 77.3 |
| 2 | Compound 2 | 285.253 | 5.0 | 8.1 | −0.511 | −1.487 | −2.118 | 0 | 37.3 |

Aqueous solubility (QP log S), octanol/water partition coefficient (QP log P), blood/brain partition coefficient (QP log BB) and human oral absorption.

**Table 3**
Effect of compound 1 and 2 on docking directed proteins GSK 3β and Insulin Receptor.

| Sample | Glycogen Synthase Kinase 3βInhibition effect Geometric Mean (MFI) | Insulin Receptor binding ability through insulin-FITCGeometric Mean (MFI) |
|---|---|---|
| Control (Untreated) | 23.54±0.53 | 12.12±0.44 |
| Compound 1 (30 μg) | 20.80±0.88 | 12.45±0.54 |
| Compound 1 (60 μg) | 25.66±0.55 | 13.60±0.22 |
| Compound 2 (100 μg) | 22.00±0.70 | 12.64±0.76 |
| Compound 2 (200 μg) | 23.96±0.94 | 11.28±0.22 |
| Metformin (10 mM) | 23.75±0.82 | 13.43±0.88 |
| Metformin (20 mM) | 25.23±0.76 | 13.82±0.44 |

MFI- Mean Fluorescent Intensity; The results were expressed as Mean ± SD; FITC-Fluorescent isothiocyanate.

## 4. Discussion

The characterization of the compounds was done by using FT-IR and NMR spectroscopic techniques. Both the effective elution with purity was undertaken for structure elucidation. The IR spectral band of compound 1 showed the band at 1692cm$^{-1}$, which revealed that the compound contained the lactone group. The characteristic absorption band corresponding to the presence of the C—O group was observed at 1330cm$^{-1}$. The broadband was observed at 3402cm$^{-1}$ corresponding to the –OH group. The infrared spectroscopic analysis of isolated compound 2 showed broadband at 3483cm$^{-1}$ corresponding to the –OH group and a sharp band observed at 3221cm$^{-1}$ due to an NH stretching. The bands observed at 1684cm$^{-1}$ and 1647cm$^{-1}$ corresponded to the C=O group and C=N group, respectively (Kalaiarasi et al., 2021). The aromatic and aliphatic CH stretching was observed in the expected region in both compounds.

The $^{1}$H—NMR spectroscopic technique revealed the presence of one broad singlet at the most downfield value δ 12.19 ppm for the proton attached to an oxygen atom in compound 1. Broad singlet observed at δ 9.16 and δ 8.81 ppm corresponding to the OH group. Multiplets observed at δ 6.63–7.31 assigned to the aromatic protons. A sharp singlet was observed at δ 2.58 ppm due to the methoxy group. In compound 2, one broad singlet at δ 12.85 ppm corresponds to the acid group proton. The multiplet observed at δ 6.65–6.83 ppm was assigned to the aromatic protons. Two aromatic -OH protons were observed at δ 4.89 ppm. Two aliphatic -OH protons were observed at δ 4.03 ppm. Two singlets observed at δ 3.68 and δ 3.71 ppm were assigned to methylene group protons (Yusufzai et al., 2017). A singlet was observed at δ 3.34 ppm assigned to the CH protons coupled with -OH proton. In addition, CH proton exhibited a singlet at δ 2.73 ppm.

The $^{13}$C—NMR spectroscopic analysis of isolated compound 1 showed signals corresponded to all the carbons in the compound. Signals at δ 183.91 ppm could be assigned to the C=O group. The methoxy carbon was found to resonate upfield at δ 63.26 ppm. The peak corresponding to the C—OH group was observed at δ 167.91, δ 165.73, δ 163.35 and δ 152.25 ppm. The rest of the aromatic carbons were found to resonate in the expected region. In compound 2, signals at δ 67.03 and δ 71.36 ppm could be assigned to the C—O group. The CH—OH carbon was found to resonate at δ 65.94 and δ 74.56 ppm, whereas C—OH carbon was found to resonate at δ 159.98 and δ 163.39 ppm. Signals at δ 168.68 could be assigned to COOH carbon and aliphatic CH carbons were observed in the expected region (Gohari et al., 2003). Based on the spectral data, the compound 1 is 5, 7-dihydroxy-2-(4-hydroxyphenyl)−3-methoxy-4*H*-chromen-4-one and compound 2 is (2,6-dihydroxypyridin-4-yl) (3,5-dihydroxytetrahydro-2*H*-pyran-4-yl) which have been confirmed by evaluating the position of chemical groups.

The compounds images are shown in Figs. 1 and 2. Compound 1 (Isokaempheride) is a flavone which were isolated from different plants and reported such as rhizomes of *Zingiber aromaticum, Z. zerumbet*, and *Sansevieria Hyacinthoides* (Chien et al., 2008; Sultana et al., 1970; Usia et al., 2004) and proved as a potent anticancer drug (Chuang et al., 2013). The prior researchers emphasized the pharmacological properties of the compound Isokaempferide which is also supporting the importance of present findings. Hence, the present protocol is a new and easy way to get a greater quantity of isokeampferide from *A. alnifolia* (14 mg/g acetone extract) by column chromatography.

Puerarin is the major bioactive ingredient isolated from the root of Pueraria lobata (Willd.) Ohwi, which is well known as Gegen in traditional Chinese medicine. Puerarin has been proved to be effective on Type II diabetes mellitus (Dong et al., 2018). Puerarin (7,4′-dihydroxy-8-C-glucosylisoflavone) belongs to the chemical structure of isoflavones. B ring is influenced by the stereo-hindrance of carbonyl group of pyran ring, which forms a large conjugate system to be an approximate planar structure in space (Zhang, 2019). These previous reports piercing the prominence of flavonoids on diabetes, also supports the present study where the flavone from *A. alnifolia* to its role on glucose homeostasis in liver cells.

One hypothesis that has been widely subjugated in conventional therapy as well as in research reports is synergistic interaction and their associated advantages or multi-factorial effects between compounds present in herbal extracts (Aiyegoro and Okoh, 2009). But in present study compound 1(67,362.66 μg Trolox eq./g extract) have more ABTS$^{+}$ radical scavenging ability than acetone extract (source extract of the compound) (39,854.17 μg Trolox eq./g extract) shows that compound 1 may inhibited by other compounds or interactions within the complex of compounds in crude form. Compounds with the least glide score would have the ability to make a maximum number of hydrogen bonds with the active site residues (Pande and Ramos, 2005). Hence in present study the least glide score and number of hydrogen bonds were considered to have more binding affinity with the target. A minimum three-point attachment of a drug to a receptor site is desired for substantial molecular reactions. A ligand may activate or inactivate its receptor which is determined by its chemical structure. GSK-3β protein is known for phosphorylation and inactivation of glycogen synthase, which acts as a negative regulator in the hormonal control of glucose homeostasis (Hazarika et al., 2012). In present findings, compound 2 has bound with GSK 3β by 4 hydrogen bonds; their G-score was −8.19 and G-energy −36.89 kcal/mol.

PPAR-α expressed in the liver, heart, and to a lesser extent, skeletal muscle and their activation promotes fatty acid oxidation, ketone body synthesis, and glucose sparing. PPAR-γ is expressed in adipose tissue, lower intestine, and cells involved in immunity (Ferré, 2004). In the present study, compound 1 is interacted well with PPAR γ by 4 hydrogen bonds. Their G-score is −8.04 and G-energy −41.91 kcal/mol. This is the best interaction between compound 2 and Glibenclamide.

Insulin receptor is considered important signal cascade for diabetic treatment and in metabolism, insulin binds to the receptor protein on the cell surface and instructs the cell to take up glucose from the blood for use as an energy source (https://www.wehi.edu.au/insulin-receptor-and-type-2-diabetes- Maja Divjak, 2015). In present binding prediction the compound 1, 2 and Glibenclamide shows good IR binding as 4,6,3 HB respectively.

Drug-likeness is a qualitative concept used in drug design to predict how drug-like a substance is. An effective drug should have optimal solubility in both water and fat. Orally administered drugs must pass through the intestinal lining, be transported in aqueous blood, and then penetrate the cellular lipid membrane to reach the inside of a cell. These result concludes that the compounds are coming under Lipinski rules and being the best suitable agent for drug development.

Researchers have been focusing on GSK-3β as a central negative regulator in the insulin signaling pathway, its role in insulin resistance, and the utility of GSK-3β inhibitors for intervention and control of metabolic diseases, including type-2 diabetes (Wagman et al., 2005). In response to insulin, the enzyme activity of GSK-3β is inhibited through Akt-mediated phosphorylation. Metformin, the most widely prescribed insulin-sensitizing agent in current clinical use, improves glucose homeostasis mainly by improving insulin-mediated suppression of hepatic glucose production associated with several mechanisms, including increased insulin receptor tyrosine kinase activity, enhanced glycogen synthesis and an increase in the recruitment and activity of GLUT4 glucose transporters (Giannarelli et al., 2003). From a scientific report, Tillandsia usneoides plant have been used for control of diabetes, the isolated compound 5, 7, 4′-trihydroxy-3, 6, 3′, 5′-tetramethoxyfllavone increases the mobilization of GLUT4 in C2C12 myoblasts and primary hepatocytes (Miranda-Nunez et al., 2021).

In the present study, the lower doses of isolated compounds are being better agent of GSK 3β inhibitors which were compared with untreated and metformin (10 mM). The inhibition of GSK 3β was observed by the peak moving towards the left and intensity value of florescence emitted by the GSK 3β-FITC. Compound 1 (30 μg) was efficiently reduced the GSK 3β level (20.80MFI) than compound 2 (30 μg) [22.00 Mean Fluorescent Intensity (MFI)]. The other dose 60 μg of compound 1, 200 μg of compound 2, and metformin higher dose were enhanced the fluorescence shows increased the expression of GSK 3β. It indicates that though the compounds are less toxic the higher concentration of compounds hinders their efficacy towards the inhibition of GSK 3β expression in present study.

Previously, Didymin is a naturally occurring orally active flavonoid glycoside (isosakuranetin 7-O-rutinoside) found in various citrus fruits which significantly increased glucose uptake in insulin-resistant HepG2 cells and decreased the expression of PTP1B in insulin-resistant HepG2 cells. In addition, didymin activated insulin receptor substrate (IRS)−1 by increasing phosphorylation at tyrosine 895 and enhanced the phosphorylations of phosphoinositide 3-kinase (PI3K), Akt, and glycogen synthasekinase-3(GSK-3) (Ali et al., 2019).

Insulin signaling initiation by the binding of insulin to the extracellular

α-subunits of the heterotetrameric Insulin Receptor (IR) made conformational changes and facilitated the autophosphorylation of tyrosine residues on the intracellular part of β-subunits (Evans, 2012). These phosphotyrosines then attract the family of insulin receptor substrates (IRS) responsible for activating PI3K (Phosphoinositide 3-kinases), MAPK (Mitogen-Activated Protein Kinase), and PKB and inhibiting the GSK-3β. The glycogen synthesis has been facilitated by the interaction of compounds at IR and GSK-3β. Ultimately, the activation of this pathway results in an enhanced translocation of the insulin-responsive GLUTs to the plasma membrane, and the increased glucose uptake in the skeletal muscle and adipose tissue (Czech, 2017). Current observation excited about the IR binding enhancement efficacy is concentration dependent in case of compound 1 and concentration independent/concentration non-reciprocal in case of compound 2. Hence the present study concludes compound 1 through IR interaction and compounds 1 & 2 through GSK-3β inhibition could maintain glucose homeostasis. These compounds are the perfect drug to mitigate the blood glucose level efficiently.

In glycogen metabolism, glycolysis and gluconeogenesis have been controlled in the liver by lowering the concentration and activation of hormones and glucose. The changes in glycogen metabolism occur by phosphorylation and dephosphorylation of glycogen phosphorylase and glycogen synthase catalyzed protein kinases and protein phosphatases (Hers, 1990). GSK-3β acts as a downstream regulatory switch that determines the output of numerous signaling pathways initiated by diverse stimuli such as Mitogen-activated protein kinase (MAPK) and AKT ((Frame and Cohen, 2001). Phosphorylation of GSK-3β (Ser9) leads to the dephosphorylation of substrates, including glycogen synthase deactivation. These findings identified GSK-3β as a vital determinant in physiological and pathological conditions, such as glycogen metabolism, insulin signaling, cell fate, neuronal function, and oncogenesis (Nakada et al., 2011; Sylow et al., 2013).

Compound 1 interacting and sensitizing the insulin receptors where the insulin binds and activates the insulin receptor tyrosine kinase, which phosphorylates and recruits different substrate adaptors including the IRS family. Among them, PI3K has a prominent role in insulin function, mainly via the activation of the AKT/PKB (Protein kinase). Activated PKB induces glycogen synthesis through inhibition of GSK-3β as well as GLUT4 translocation. Here, compound 1 interaction inhibiting the GSK-3β significantly also through the phosphorylation of MAPK. In another way, a lower concentration of compounds 1 and 2 interacted with GSK 3β directly or indirectly inhibiting and at their higher concentration it assisted for the expression. The abovesaid possible molecular interactions of compounds in liver glucose homeostasis is exhibited in Fig. 3.

The two main precautionary approaches in metabolic syndrome management are primarily the lifestyle modifications, food habits that restore energy balance by reducing calorie intake and secondarily increased energy expenditure by physical activity and pharmaceutical interventions (Ford et al., 2010; Grundy et al., 2004). With adore this hypothesis, the wild leafy vegetable *A. alnifolia* will be one of the dietary supplements for diabetic patients as “Food being the Medicine”.

## 5. Conclusion

The plant *Acalypha alnifolia* was reported for numerable traditional importance, based on which efficacy of the plant have been traced through various *in-vitro* and *in-vivo* researches. In the present study, the acetone extract of *A. alnifolia* is focused to invent active compounds and their molecular interactions with diabetic protiens. The flavone compound Isokaempferide (compound 1) and an alkaloid (compound 2) is extracted and purified. The presence of Isokaempferide in *A. alnifolia* has been revealed and makes to know the availability of the compound as an alternative source and novel method of isolation is expounded for better accessibility (Granted patent/ Indian patent/No. 349229). The another compound pyridine alkaloid (compound 2) was also reported in the present study is the new compound in alkaloid group reported first time in this plant *A. alnifolia* and both the compounds were substantiated for glucose homeostasis in liver cells were revealed by GSK 3β inhibition and enhancing the insulin binding capability. The present study illuminated the plant potential which will aid in active drug development for diabetes management.

This study also suggested that the extraction and evaluation of

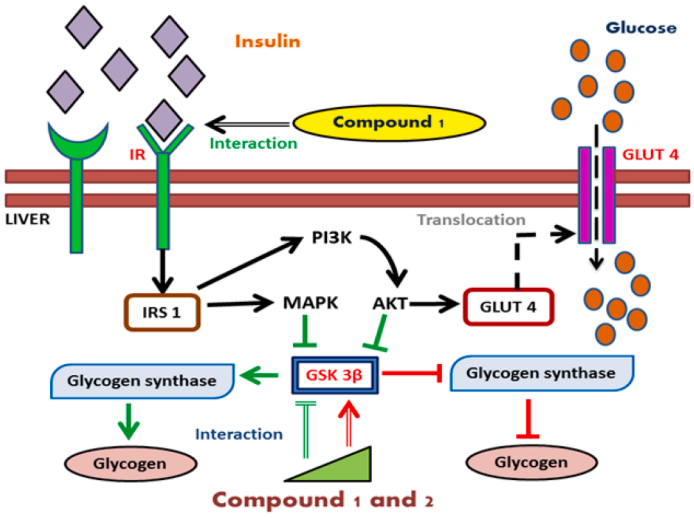


**Fig. 3.** Effect of compound 1 and 2 in glucose homeostasis. Compound 1 might be interacted with IR and help to sensitize the receptors. Activated AKT/PKB through PI3K or direct activation of MAPK induces glycogen synthesis through inhibition of GSK-3β as well as GLUT 4 translocation.

pharmaceutical properties of leftover active compounds of *A. alnifolia* are required in future research. As per the direction of docking results, the PPAR and GLUT 4 expression studies are essential to analyze the noble mechanism of isolated compounds. In addition to that, the awareness on wild leafy vegetable *A. alnifolia* to get in the form of nutraceuticals, to analyze the cultivation strategies and encouragement for commercialization would be the best approaches with the plant to accomplish diabetes prevention and management.

## CRediT authorship contribution statement

**Revathi Ponnusamy:** Visualization, Methodology, Writing – review & editing. **Kalaiarasi Giriraj:** Visualization, Methodology, Writing – review & editing. **Magesh Selvakumar AM:** Formal analysis. **Parimelazhagan Thangaraj:** Visualization, Methodology, Writing – review & editing. **Saikumar Sathyanarayanan:** Visualization, Writing – review & editing. **Adriano Antunes de Souza Araújo:** Writing – review & editing, Conceptualization, Data curation. **Saravanan Shanmugam:** Writing – review & editing, Conceptualization, Data curation. **Lucindo José Quintans Junior:** Writing – review & editing, Conceptualization, Data curation.

## Declaration of Competing Interests

The authors declare that they have no known competing financial interests or personal relationships that could have appeared to influence the work reported in this paper.

## Acknowledgments

The author Dr. P. Revathi likes to acknowledge the Department of Science and Technology (DST), India for the grant as in the form of INSPIRE fellowship (Grant No: IF120011) during the research.

## Supplementary materials

Supplementary material associated with this article can be found, in the online version, at doi:10.1016/j.phyplu.2022.100216.

## References

Aiyegoro, O.A., Okoh, A.I, 2009. Use of bioactive plant products in combination with standard antibiotics: implications in antimicrobial chemotherapy. J. Med. Plant Res. 3, 1147–1152.
Agrawal, M., Agrawal, Y., Itankar, P., Patil, A., Vyas, J., Kelkar, A., 2012. Phytochemical and HPTLC studies of various extracts of annona squamosa (Annonaceae). Int. J. Pharm. Tech. Res. 4 (1), 364–368.
Balakrishnan, V., Prema, K., Ravindran, J., 2009. Ethnobotanical studies among villagers From Dharapuram Taluk. Tamil Nadu, India.
Blois, M.S., 1958. Antioxidant determinations by the use of a stable free radical. Nature 181, 1199–1200. https://doi.org/10.1038/1811199a0.
Chien, T.Y., Chen, L.G., Lee, C.J., Lee, F.Y., Wang, C.C., 2008. Anti-inflammatory constituents of Zingiber zerumbet. Food Chem. 110, 584–589. https://doi.org/10.1016/j.foodchem.2008.02.038.
Chuang, K.A., Lieu, C.H., Tsai, W.J., Huang, W.H., Lee, A.R., Kuo, Y.C., 2013. 3-Methoxyapigenin modulates β-catenin stability and inhibits Wnt/β-catenin signaling in Jurkat leukemic cells. Life Sci. 92, 677–686. https://doi.org/10.1016/j.lfs.2012.12.007.
Czech, M.P., 2017. Insulin action and resistance in obesity and type 2 diabetes. Nat Med 23, 804–814. Liver Tox: Clinical and Research Information on Drug-Induced Liver Injury [Internet]. Bethesda (MD): National Institute of Diabetes and Digestive and Kidney Diseases; 2012-. Antidiabetic Agents. [Updated 2017 Jun 6]. Available from: https://www.ncbi.nlm.nih.gov/books/NBK548783/.
DeFronzo, R.A., Eldor, R., Abdul-Ghani, M., 2013. Pathophysiologic approach to therapy in patients with newly diagnosed type 2 diabetes. Diabetes Care 36, S127–S138.
Evanjelene, V.K., Natarajan, D., 2012. In vitro and in vivo antioxidant analysis of Acalypha alnifolia Klein ex. Acta Biol. Indica 99–103.
Evans, M., 2012. Diabetes mellitus, insulin, oral antidiabetes agents, obesity. Clinical Pharmacology: Eleventh Edition. Elsevier Inc., pp. 572–586. https://doi.org/10.1016/B978-0-7020-4084-9.00075-6
Ferré, P., 2004. The Biology of Peroxisome Proliferator-Activated Receptors: Relationship with Lipid Metabolism and Insulin Sensitivity, in: Diabetes. Diabetes Association Inc, American. https://doi.org/10.2337/diabetes.53.2007.s43.
Ford, E.S., Li, C., Zhao, G., 2010. Prevalence and correlates of metabolic syndrome based on a harmonious definition among adults in the US. J. Diabetes 2, 180–193. https://doi.org/10.1111/j.1753-0407.2010.00078.x.
Frame, S., Cohen, P., 2001. GSK3 takes centre stage more than 20 years after its discovery. Biochem. J. https://doi.org/10.1042/0264-6021:3590001.
Giannarelli, R., Aragona, M., Coppelli, A., Del Prato, S., 2003. Reducing insulin resistance with metformin: the evidence today. Diabetes Metab. https://doi.org/10.1016/s1262-3636(03)72785-2.
Gohari, A.R., Saeidnia, S., Matsue, K., Uchiyama, N., Yagura, T., Ito, M., Kiuchi, F., Honda, G., 2003. Flavonoid constituents of dracocephalum kotschyi growing in Iran and their trypanocidal activity. J. Nat. Med. 57 (6), 250–252.
Grundy, S.M., Brewer, H.B., Cleeman, J.I., SmithLenfant, S.C.C., 2004. Definition of metabolic syndrome: report of the National Heart, Lung, and Blood Institute/American Heart Association conference on scientific issues related to definition., in: Arteriosclerosis, Thrombosis, and Vascular Biology. Arterioscler Thromb Vasc Biol. https://doi.org/10.1161/01.ATV.0000111245.75752.C6.
Hazarika, R., Parida, P., Neog, B., Yadav, R., 2012. Binding energy calculation of GSK-3 protein of human against some anti-diabetic compounds of Momordica charantia

linn (Bitter melon). Bioinformation 8, 251–254. https://doi.org/10.6026/97320630008251.
Hers, H.G., 1990. Mechanisms of blood glucose homeostasis. J. Inherit. Metab. Dis. 13, 395–410. https://doi.org/10.1007/BF01799497.
Han, H.-S., Kang, G., Kim, J.S., Choi, B.H., Koo, S.-H., 2016. Regulation of glucose metabolism from a liver-centric perspective. Exp. Mol. Med. 48 e218.
Panchal, I.I., Sen, D.J., Patel, AD., Shah, U., et al., 2018. Molecular docking, synthesis and biological evaluation of sul-phonylureas/guanidine derivatives as promising antidiabeticagent. Curr. Drug Discov. Technol. 15, 315–325.
Miranda-Nuñez, J.E., Zamilpa-Alvarez, A., Fortis-Barrera, A., Alarcon-Aguilar, F.J., Loza-Rodriguez, H., Gomez-Quiroz, LE., Salas-Silva, S., Flores-Cruz, M., Zavala-Sanchez, M.A., Blancas-Flores, G., 2021. GLUT4 translocation in $C_2C_{12}$ myoblasts and primary mouse hepatocytes by an antihyperglycemicflavone from Tillandsia usneoides. Phytomedicine 89.
Johnkennedy, N., Adamma, E., Nnedimma, N.C., 2011. Hypolipidemic effects of aqueous extract of Acalypha capitata leaves in rats fed on high cholesterol diet. Asian Pac. J. Trop. Biomed. 1 https://doi.org/10.1016/S2221-1691(11)60152-4. S183–S185.
Kalaiarasi, G., Dharani, S., Rex Jeya Rajkumar, Ranjani, S.M., Vincent, L.M., Prabhakaran, R., 2021. Synthesis, spectral characterization, DNA/BSA binding, antimicrobial and in vitro cytotoxicity of cobalt(III) complexes containing 7-hydroxy-4-oxo-4H-chromene Schiff bases. Inorg. Chim. Acta 515, 120060.
KhanYusufzai, S., Osman, H., Shaheen Khan, M., Mohamad, S., Sulaiman, O., Parumasivam, T., Azlan Gansau, J., Johansah, N., Noviany, E., 2017. Design, characterization, in vitro antibacterial, antitubercular evaluation and structure–activity relationships of new hydrazinyl thiazolyl coumarin derivatives. Med. Chem. Res. 26, 1139–1148.
Lankatillake, C., Huynh, T., Dias, D.A., 2019. Understanding glycaemic control and current approaches for screening antidiabetic natural products from evidence-based medicinal plants. Plant Methods 15, 105.
Zhang, L., 2019. Pharmacokinetics and drug delivery systems for puerarin, a bioactive flavone from traditional Chinese medicine. Drug Deliv. 26 (1), 860–869.
Lipinski, B., 2001. Pathophysiology of oxidative stress in diabetes mellitus. J. Diabetes Complicat. 15, 203–210. https://doi.org/10.1016/S1056-8727(01)00143-X.
Lipinski, C.A., Lombardo, F., Dominy, B.W., Feeney, P.J., 2001. Experimental and computational approaches to estimate solubility and permeability in drug discovery and development settings. Adv. Drug Deliv. Rev. 46, 3–26.
Ali, MdY, Zaib, S., Mizanur Rahman, M., Jannat, S., Iqbal, J., Park, S.K., Chang, M.S., 2019. Didymin, a dietary citrus flavonoid exhibits anti-diabetic complications and promotes glucose uptake through the activation of PI3K/Akt signaling pathway in insulin-resistant HepG2 cells. Chem. Biol. Interact. 305, 180–194.
Mohamed, J., Nazratun Nafizah, A.H., Zariyantey, A.H., Budin, S.B., 2016. Mechanisms of Diabetes-Induced Liver Damage: the role of oxidative stress and inflammation. Sultan Qaboos Univ. Med. J. 16 (2) e132–e141.
Meneses, M.J., Silva, B.M., Sousa, M., Sá, R., Oliveira, P.F., Alves, M.G., 2015. Antidiabetic drugs: mechanisms of action and potential outcomes on cellular metabolism. Curr. Pharm. Des. 21 (25), 3606–3620.
Melan, M.A., 1999. Overview of cell fixatives and cell membrane permeants. Methods Mol. Biol. https://doi.org/10.1385/1-59259-213-9:45.
Mosmann, T., 1983. Rapid colorimetric assay for cellular growth and survival: application to proliferation and cytotoxicity assays. J. Immunol. Methods 65, 55–63. https://doi.org/10.1016/0022-1759(83)90303-4.
Nabben, M., Neumann, D., 2016. GSK-3 inhibitors: anti-diabetic treatment associated with cardiac risk? Cardiovasc. Drugs Ther. 30, 233–235.
Nakada, M., Minamoto, T., Hayashi, I.V.Y., Ham, J., 2011. The pivotal roles of GSK3β in glioma biology, in: Molecular Targets of CNS Tumors. InTech. https://doi.org/10.5772/21458.
Pande, V., Ramos, M., 2005. Nuclear factor Kappa B: a potential target for Anti-HIV chemotherapy. Curr. Med. Chem. 10, 1603–1615. https://doi.org/10.2174/0929867033457250.
Pagadala, N.S., Syed, K., Tuszynski, J. (2017). Software for molecular docking: a review. Biophysical reviews, 9(2), 91–102. Kim S. Getting the most out of PubChem for virtual screening. Expert Opin Drug Discov. 2016 Sep;11(9):843-55.
Ponnusamy, R., Thangaraj, P., 2014. Total nutritional capacity and inflammation inhibition effect of Acalypha alnifolia Klein ex wild - An unexplored wild leafy vegetable. J. Food Drug Anal. 22, 439–447. https://doi.org/10.1016/j.jfda.2014.04.004.
Popova, I.E., Hall, C., Kubátová, A., 2009. Determination of lignans in flaxseed using liquid chromatography with time-of-flight mass spectrometry. Journal of Chromatography A 1216 (2), 217–229.
Qiang, G., Xue, S., Yang, J.J., Du, G., Pang, X., Li, X., Goswami, D., Griffin, P.R., Ortlund, E.A., Chan, C.B., Ye, K., 2014. Identification of a small molecular insulin receptor agonist with potent antidiabetes activity. Diabetes 63, 1394–1409. https://doi.org/10.2337/db13-0334.
Re, R., Pellegrini, N., Proteggente, A., Pannala, A., Yang, M., Rice-Evans, C., 1999. Antioxidant activity applying an improved ABTS radical cation decolorization assay. Free Radic. Biol. Med. 26, 1231–1237.
Revathi, P., Parimelazhagan, T., 2015a. Anti-diabetic analysis and insulin expression study of a wild leafy vegetable acalypha alnifolia klein ex wild. On streptozotocininduced diabetic rats. Bangladesh J. Pharmacol. 10, 461–466. https://doi.org/10.3329/bjp.v10i2.21931.
Revathi, P., Parimelazhagan, T., 2015b. Anti-diabetic analysis and insulin expression study of a wild leafy vegetable acalypha alnifolia klein ex wild. On streptozotocininduced diabetic rats. Bangladesh J. Pharmacol. 10, 461–466. https://doi.org/10.3329/bjp.v10i2.21931.
Revathi, P., Parimelazhagan, T., Manian, S., 2013. Quantification of phenolic compounds, *in vitro* antioxidant analysis and screening of chemical compounds. Int. J. Pharm. Bio Sci. 4, 973–986.
Sepidarkish, M., et al., 2020. Effects of Melissa officinalis (Lemon Balm) on cardio-metabolic outcomes: a systematic review and metaanalysis. Phytother. Res. 1–11. https://doi.org/10.1002/ptr.6744.
Sharfi, H., Eldar-Finkelman, H., 2008. Sequential phosphorylation of insulin receptor substrate-2 by glycogen synthase kinase-3 and c-Jun NH2-terminal kinase plays a role in hepatic insulin signaling. Am. J. Physiol. Endocrinol. Metab. 294. E307–E315.
Sultana, N., Rahman, M., Ahmed, S., Akter, S., Haque, M., Parveen, S., Moeiz, S., 1970. Antimicrobial compounds from the rihzomes of sansevieria hyacinthoides. Bangladesh J. Sci. Ind. Res. 46, 329–332. https://doi.org/10.3329/bjsir.v46i3.9038.
Suzuki, T., Bridges, D., Nakada, D., Skiniotis, G., Morrison, S.J., Lin, J.D., et al., 2013. Inhibition of AMPK catabolic action by GSK3. Mol. Cell 50, 407–419.
Sylow, L., Jensen, T.E., Kleinert, M., Mouatt, J.R., Maarbjerg, S.J., Jeppesen, J., Prats, C., Chiu, T.T., Boguslavsky, S., Klip, A., Schjerling, P., Richter, E.A., 2013. Rac1 is a novel regulator of contraction-stimulated glucose uptake in skeletal muscle. Diabetes 62, 1139–1151. https://doi.org/10.2337/db12-0491.
Thangaraj, P., 2016. Pharmacological Assays of Plant-Based Natural Products. Springer International Publishing, Switzerland, pp. 177–180.
Usia, T., Iwata, H., Hiratsuka, A., Watabe, T., Kadota, S., Tezuka, Y., 2004. Sesquiterpenes and flavonol glycosides from Zingiber aromaticum and their CYP3A4 and CYP2D6 inhibitory activities. J. Nat. Prod. 67, 1079–1083. https://doi.org/10.1021/np030556a.
Bajpai, V.K., Majumder, R., Park, J.G., 2016. Isolation and purification of plant secondary metabolites using column-chromatographic technique. Bangladesh J. Pharmacol. 11, 844–848.
Wagman, A., Johnson, K., Bussiere, D., 2005. Discovery and development of GSK3 inhibitors for the treatment of type 2 diabetes. Curr. Pharm. Des. 10, 1105–1137. https://doi.org/10.2174/1381612043452668.
Amidzadeh, Z., Behzad Behbahani, A., Erfani, N., Sharifzadeh, S., Ranjbaran, R., Moezi, L., Aboualizadeh, F., Okhovat, M.A., Alavi, P., 2014. Assessment of different permeabilization methods of minimizing damage to the adherent cells for detection of intracellular RNA by flow cytometry - PubMed. Avicenna J. Med. Biotechnol. 6, 38–46.